Spin relaxation in (110) and (001) InAs/GaSb superlattices

K. C. Hall, K. Gündoğdu, E. Altunkaya, W. H. Lau, Michael E. Flatté, and Thomas F. Boggess
Department of Physics and Astronomy, Optical Science and Technology Center, The University of Iowa, Iowa City, Iowa 52242, USA

J. J. Zinck, W. B. Barvosa-Carter, and S. L. Skeith
HRL Laboratories, LLC, 3011 Malibu Canyon Road, Malibu, California 90265, USA

(Received 6 January 2003; published 19 September 2003)

We report an enhancement of the electron spin-relaxation time (T_1) in a (110) InAs/GaSb superlattice by more than an order of magnitude (25 times) relative to the corresponding (001) structure. The spin dynamics were measured using polarization sensitive pump probe techniques and a mid-infrared, subpicosecond periodically poled $LiNbO_3$ optical parametric oscillator. Longer T_1 times in (110) superlattices are attributed to the suppression of the native interface asymmetry and bulk inversion asymmetry contributions to the precessional D'yakonov Perel spin-relaxation process. Calculations using a nonperturbative 14-band nanostructure model give good agreement with experiment and indicate that possible structural inversion asymmetry contributions to T_1 associated with compositional mixing at the superlattice interfaces may limit the observed spin lifetime in the (110) superlattice under study, suggesting the possibility for further improvements in T_1 through targeted growth techniques. Our findings have implications for spintronics applications using InAs/GaSb heterostructures.

DOI: 10.1103/PhysRevB.68.115311 PACS number(s): 78.67.Pt, 78.47.+p, 72.25.Rb

Semiconductor heterostructures based on the InAs/GaSb/AlSb system have gained attention recently for potential applications in the rapidly growing field of semiconductor-based spintronics, in which the focus is to develop novel electronic devices and circuits that exploit the spin property of the electron.[1,2] By utilizing some of the unique characteristics of the InAs/GaSb/AlSb system, including the strong spin-orbit interaction in InAs and GaSb, and the resulting large Rashba coefficient[3] and electron g factor, the ability to form a variety of interface types (type-I, type-II staggered, and type-II broken gap), and the high electron mobility of InAs, it may be possible to realize a host of novel high-speed, spin-sensitive electronic devices. For instance, InAs/GaSb/AlSb heterostructures are a prime candidate for a number of recent spintronics device proposals, including Rashba spin filters,[4–6] a spin field effect transistor[7] and a high-frequency optical modulator utilizing spin precession.[8]

A crucial factor in the design of any spin-sensitive electronic device is the electron-spin-relaxation time (T_1), which must be sufficiently long to allow for transport and/or processing of the spin-polarized electrons. Due to the high electron mobility in InAs-based heterostructures, relevant device transport times can be very short. For instance, the transit time delay for electrons in a resonant tunnel device is <100 fs,[6,9] and switching transition times <1.5 ps have been achieved.[9] However, a recent measurement of the spin relaxation time in a (001) InAs/GaSb superlattice[10] indicated a value for T_1 that is of comparable magnitude to these transport times ($\leqslant 1$ ps), a finding which may impose serious limitations on device architectures. This rapid spin relaxation was attributed to dominant precessional decay associated with asymmetry in interface bonding, referred to as native interface asymmetry (NIA). NIA occurs in (001)-oriented no-common-atom semiconductor heterostructures, in which the interface bonds differ from those in the bulk constituents, leading to a strong local gradient in the potential that is asymmetric due to different bond composition or orientation at the normal and inverted interfaces.[2,10–13] In addition to affecting the band gap and intervalence band absorption properties of (001) InAs/GaSb superlattices,[11] NIA was found to dominate the contribution to precessional spin relaxation associated with bulk inversion asymmetry[14] by more than an order of magnitude.[10]

The interface contribution to spin relaxation in these no-common-atom superlattices may be removed through (110) growth, since the mixed anion-cation interface planes in this orientation lead to a symmetric interface potential. (See Fig. 1.) Since NIA strongly dominates spin relaxation in (001)-

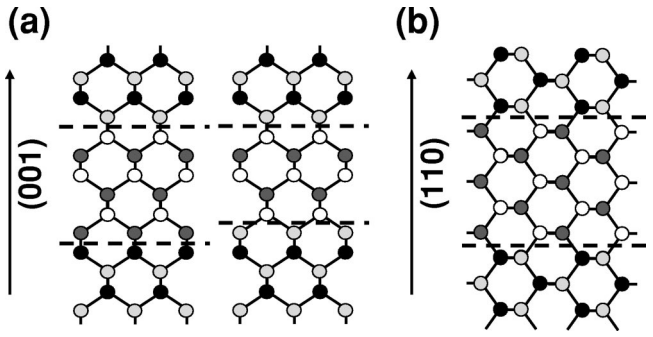

FIG. 1. Schematic diagram of the interfaces in InAs/GaSb superlattices for (a): (001) and (b): (110) directions of growth. The shades indicate, in order of increasing darkness, Sb, In, Ga, and As. Since InAs and GaSb have no atom in common, for (001) superlattices the interface potential is intrinsically asymmetric, referred to as NIA. The two types of bonding configurations for (001) superlattices are shown: different bond composition at the two interfaces (InSb and GaAs), or bonds of the same composition (InSb is shown) but different orientation. In contrast, for (110) no-common-atom superlattices, NIA is absent because the interfaces are mixed, containing equal numbers of both anions and cations, leading to a symmetric interface potential.

oriented InAs/GaSb superlattices, the electron-spin lifetime is expected to be considerably longer in (110) InAs/GaSb superlattices. Additionally, suppression of the remaining BIA contribution in (110) heterostructures has been predicted[15] and recently verified experimentally in GaAs/AlGaAs quantum wells.[16] This suppression is expected to further extend the spin lifetimes in (110)-oriented InAs/GaSb superlattices. Here we report measurement of spin-relaxation times in (110) and (001) InAs/GaSb superlattices using a mid-infrared femtosecond optical parametric oscillator and polarization sensitive differential transmission experiments. We observed an increase in T_1 by more than an order of magnitude (>25 times) for (110) growth. This enhancement in T_1 represents a critical improvement in the material characteristics of the InAs/GaSb/AlSb system for the above mentioned spintronics device concepts, and will substantially widen the scope of possible applications using this promising spintronics material. Theoretical calculations using a nonperturbative 14-band $\mathbf{k}\cdot\mathbf{p}$ nanostructure model agree well with the experiment. Our theoretical calculations suggest that T_1 in the (110) superlattice under study here may be limited by compositional mixing at the interfaces, indicating that further improvements in the spin lifetime may be achievable through control and optimization of interface characteristics using targeted growth methods.[17–21]

The InAs/GaSb superlattices were grown by molecular beam epitaxy on n-type [$1-2\times10^{16}$ cm^{-3}] (001) or (110)-oriented InAs substrates [$(+/-)$ 0.1 degree] in a Fisons VG-80 machine equipped with shuttered EPI group-III evaporators and shuttered EPI valved group-V cracker cells. The superlattice structures contain 2.1 nm thick InAs layers and 3.7-nm thick GaSb layers, with a total of 85 periods. The (110) and (001) superlattices were grown in consecutive runs to minimize differences in extrinsic sample characteristics. X-ray diffraction measurements indicate high-order resolution of the SL peaks, and features of the RHEED pattern are highly streaked, indicating good quality superlattice growth. The room temperature continuous wave photoluminescence signal from the superlattices was of similar intensity and line width for the (001) and (110) structures, and the carrier recombination time, measured by time-resolved photoluminescence up-conversion experiments, was found to be similar in the two superlattices (1–2 ns), indicating consistency of sample quality. Photoluminescence measurements provide an especially sensitive measure of interface quality in these short period InAs/GaSb superlattices due to the spatially-indirect optical transitions.

T_1 times were measured at low temperature (115 K) using pump probe experiments involving 200 fs, circularly polarized mid-infrared pulses (4.0–4.6μm). The laser source for these measurements is an optical parametric oscillator (OPO) that relies on parametric down conversion in a 1 mm thick periodically poled $LiNbO_3$ (PPLN) crystal.[22] The OPO is synchronously pumped by a Titanium sapphire oscillator, and provides 20–100 mW of average idler output power over the spectral tuning range (2.7–4.6 μm). The output pulses have a fullwidth at half maximum bandwidth of 18 meV.

The confinement-induced splitting of the band edge heavy-hole and light-hole states is calculated to be $\geqslant130$ meV for the (001) and (110) InAs/GaSb superlattices considered here. In this case, circularly polarized idler pulses tuned close to the band gap will excite only the heavy hole to conduction band transition, leading to a 100% spin-polarized distribution of electrons. The band gap of the (110) superlattice is slightly lower (≈40 meV) than the corresponding (001) structure. Electronic structure calculations using our 14-band $\mathbf{k}\cdot\mathbf{p}$ nanostructure model suggest that this difference is due to lower electron and hole confinement energies in the (110) superlattice in addition to the differing influence of strain for different directions of superlattice growth. For the experiments reported here, the OPO was tuned to 35 meV above the band gap for each structure,[23] corresponding to an electron energy of approximately 20 meV.[24] The optically injected carrier density was estimated using the measured pump pulse fluence and the calculated absorption spectrum for each structure to be 1×10^{16} cm^{-3} for (110) and 3×10^{16} cm^{-3} for (001), with an uncertainty of $\pm40\%$. The experimental complications involved in these mid-infrared experiments, including the limited pulse energy and tuning range of the OPO and the weak band edge absorption of these broken gap InAs/GaSb superlattices (≈1100 cm^{-1}) restricted the range of experimental conditions accessible in our experiments. In order to isolate a dependence of the spin lifetime on growth direction orientation for InAs/GaSb superlattices, we have compared spin lifetimes in (110) and (001) superlattices of identical layer thickness at the same lattice temperature and excess carrier energy, and for similar carrier densities. Additionally, the momentum scattering time, which influences the spin decay time as discussed below, in the nominally undoped short-period superlattices studied here will likely be determined by interface roughness scattering.[31] Although direct measurements of carrier mobility in these superlattices are prohibited due to the conducting InAs substrates on which they were grown, since the quality of our superlattices was characterized extensively through other means, yielding similar results for the (001) and (110) superlattices as described above, no significant difference in momentum scattering time between these superlattices is expected.

The optically-injected, spin-polarized electrons generate absorption bleaching of the associated interband transition through state filling. By monitoring the transmission of a weaker, delayed probe pulse that has the same (SCP) or opposite (OCP) circular polarization as the pump pulse, T_1 may be extracted. The differential transmissivity was measured versus the time delay between the pump and probe pulses using a liquid N_2-cooled InSb detector and lock-in detection methods. In our experiments, care was taken to ensure that the pump beam impinges on the superlattice sample at normal incidence. In this case, the probe beam interrogates the relaxation time of electron spins polarized in the growth direction. Fig. 2 shows the results of polarization-sensitive differential transmission measurements on InAs/GaSb superlattices with (001) [Fig. 2(a)] and (110) [Fig. 2(b)] directions of growth. Note the time scales on the x axes in Fig. 2(a) and Fig. 2(b), which differ by more than an order of magnitude. The large negative pulse-width-limited feature appearing in both data sets originates from two-photon absorption in the

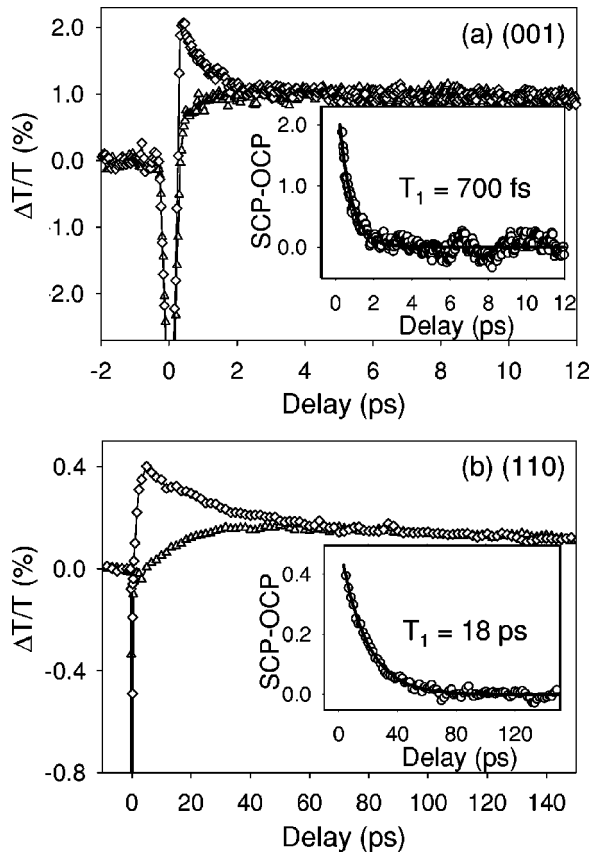

FIG. 2. Results of differential transmission experiments on InAs/GaSb superlattices with (a): (001) and (b): (110) directions of growth. Data for conditions of same circular (SCP) and opposite circular (OCP) polarization geometries are indicated by open diamonds and triangles, respectively. Note the time scales on the *x* axes in (a) and (b), which differ by more than an order of magnitude. Inset: single exponential fit to the difference between the decay curves for SCP and OCP.

InAs substrates. This feature provides a convenient marker for zero time delay, but may otherwise be ignored for the purpose of this discussion. The loss of spin polarization in the optically-injected carrier distribution is indicated by the convergence of the differential transmission signals for the SCP and OCP polarization geometries. From a comparison of the data in Fig. 2(a) and 2(b), it is clear that spin relaxation occurs on a much longer time scale in the (110) InAs/GaSb superlattice compared to the (001) structure. The OCP signal in Fig. 2(b) grows from ≈ 0, indicating that the optically excited carriers are initially fully spin polarized, and that no detectable Coulomb screening effects are present. In the data for the (001) superlattice in Fig. 2(a), the nonzero bleaching signal in the OCP data immediately following the two-photon absorption feature is evidence of spin decay during pulse overlap. T_1 times are obtained by performing a single exponential fit to the difference between the SCP and OCP curves. Fits were restricted to delay values $\geqslant 350$ fs to avoid the two-photon absorption feature. From the data in Fig. 2, we find T_1 values of 700 fs and 18 ps for the (001) and (110) superlattices respectively, indicating that the spin-relaxation time in InAs/GaSb superlattices, is strongly enhanced with (110) growth. These lifetimes were not found to vary significantly over the restricted range of accessible temperatures for these experiments (77–115 K).

The much longer spin lifetime in the (110) InAs/GaSb superlattice relative to the corresponding (001) structure is primarily attributed to the elimination of the NIA contribution to spin relaxation. Although a larger T_1 is expected in (110) superlattices due to suppression of the BIA contribution,[15] for the short period no-common-atom superlattices investigated here the more crucial distinction arises from the nature of the interfaces. Figure 1 contains a schematic diagram of the interfaces in InAs/GaSb superlattices for conditions of growth along the (001) [Fig. 1(a)] and (110) [Fig. 1(b)] directions. For the (001) superlattice, the potential at the interfaces is asymmetric due to tetrahedral bonding between the bulk constituents (InAs and GaSb) that share no atom in common. This effect is referred to as NIA. As in the case of BIA, NIA generates a pseudomagnetic field that serves to relax the electron spins. It has been shown previously[10] that NIA strongly dominates the electron spin decay process in a similar (001)-oriented InAs/GaSb superlattice grown on a GaSb substrate. The subpicosecond spin lifetime extracted from the data of Fig. 2(a) is consistent with these earlier studies.[10] In contrast, for an InAs/GaSb superlattice grown in the (110) direction, NIA is absent because the interfaces are mixed, containing equal numbers of both anions and cations [see Fig. 1(b)]. In this case, the interface potential is symmetric. Since spin decay in the (001) superlattice is strongly dominated by NIA, with its elimination in the (110) structure the spin lifetime is expected to sharply increase, consistent with the results in Fig. 2(b).

In order to interpret these findings, we have performed calculations of spin relaxation times due to the precessional D'yakonov Perel mechanism, which has been found to dominate in III–V semiconductors and their heterostructures for temperatures above 77 K.[2,10,14,25–30] We employ a nonperturbative $\mathbf{k}\cdot\mathbf{p}$ nanostructure model solved in a 14-band restricted basis set, in which BIA contributions are included naturally[14] and NIA contributions are introduced as previously described.[10] Parameters governing the interface asymmetry were taken from Ref. 10. Neutral impurities were taken as the dominant source of momentum scattering. The spin lifetime varies inversely with momentum scattering time, $T_1 \sim \tau_p^{-1}$. We find good agreement with experiment using $\tau_p = 190$ fs, which is within the typical range (100–200 fs) for the III–V semiconductors, including measurements on similar InAs/GaInSb superlattices.[31]

The calculated spin relaxation time for the (001) superlattice is $T_1 = 715$ fs in good agreement with the experimental value of 700 fs. NIA was found to strongly dominate the electron spin-relaxation process for the (001) structure, consistent with earlier findings.[10] For the (110) InAs/GaSb superlattice, our calculations indicate that, with the elimination of NIA and the strong suppression of the remaining BIA contribution,[15] the spin lifetime is expected to be ~ 600 ps. This lifetime is limited by the small, in-plane component of the BIA crystal magnetic field that arises from contributions beyond third order in the electron wavevector, which are included naturally within the 14-band nonperturbative theo-

retical treatment used here.[14] The much shorter T_1 observed experimentally (18 ps) indicates that additional contributions to the spin relaxation process are present and substantially dominate over BIA. The electron-hole exchange interaction [the Bir-Aronov-Pikus mechanism[32](BAP)] is not a favorable candidate to account for the measured spin lifetime in the (110) superlattice due to the small electron-hole overlap[33,34] characteristic of these broken-gap InAs/GaSb superlattices (roughly 20% compared to GaAs/AlGaAs quantum wells) and because the timescale of spin decay (18 ps) is much shorter than that found previously for the BAP interaction.[16,25] The Elliott-Yafet mechanism,[35,36] which increases in importance with decreasing band gap,[25,37] may limit T_1 in (110) InAs/GaSb superlattices, although a detailed theoretical treatment for this mechanism in III–V semiconductor superlattices is not presently available.

Because of the large spin-orbit interaction and small band gap in InAs/GaSb superlattices, a substantial contribution to the spin decay process could arise from a small degree of structural inversion asymmetry (SIA) associated with compositional mixing at the superlattice interfaces. In order to assess the sensitivity of T_1 to such effects, the spin lifetime was calculated assuming that the interface on one side of the InAs layers is not compositionally abrupt, corresponding to a *single monolayer* of $In_{0.5}Ga_{0.5}As_{0.5}Sb_{0.5}$. Such a situation may arise due to differing growth kinetics at the normal and inverted interfaces, an effect that commonly occurs in (001) InAs/GaSb superlattices and has been extensively studied using cross-sectional scanning tunneling microscopy and other techniques.[38–41] With the inclusion of the mixed composition monolayer, the calculated spin lifetime in the (110) InAs/GaSb superlattice was reduced by a factor of 20, yielding a value of 29 ps, in line with the experimental value of 18 ps. This dramatic reduction in T_1 occurs because, although the pseudomagnetic field associated with BIA is primarily in the growth direction for (110)-oriented superlattices, SIA introduces a field component in the plane of the superlattice that serves to relax the growth-direction polarized electron spins injected in these optical experiments. In contrast, for the (001)-oriented superlattice including such compositional mixing has a much smaller influence on the calculated spin lifetimes because, for (001) superlattices, both the psuedomagnetic fields associated with BIA[15] and NIA have large in-plane components. Detailed *STM* characterization of the present (110) superlattice would help in the conclusive identification of the physical process limiting T_1.

In summary, we observe an enhancement of the electron spin relaxation time in InAs/GaSb superlattices by more than an order of magnitude (>25 times) with (110)-oriented growth using polarization sensitive pump probe techniques and a mid-infrared, subpicosecond PPLN OPO. This enhancement is attributed to suppression of the NIA and BIA contributions to the spin decay process in (110) superlattices. Our findings will substantially widen the scope of possible applications using this promising spintronics material.

This research was supported by the DARPA grant no. MDA972-01-C-0002, grant no. DARPA/ARO DAAD19-01-1-0490 and the Natural Sciences and Engineering Research Council of Canada.

[1] S.A. Wolf *et al.*, Science **294**, 1488 (2001).
[2] *Semiconductor Spintronics and Quantum Computation*, edited by D.D. Awschalom, D. Loss, and N. Samarth (Springer-Verlag, Berlin, 2002).
[3] X. Cartoixa, D.Z.Y. Ting, E.S. Daniel, and T.C. McGill, Superlattices Microstruct. **30**, 309 (2001).
[4] A. Voskoboynikov, Shiue Shin Lin, C.P. Lee, and O. Tretyak, J. Appl. Phys. **87**, 387 (2000).
[5] T. Koga, J. Nitta, H. Takayanagi, and S. Datta, Phys. Rev. Lett. **88**, 126601 (2002).
[6] D.Z.-Y. Ting and X. Cartoixa, Appl. Phys. Lett. **81**, 4198 (2002).
[7] S. Datta and B. Das, Appl. Phys. Lett. **56**, 665 (1990).
[8] S. Hallstein, J.D. Berger, M. Hilpert, H.C. Schneider, W.W. Rühle, F. Jahnke, S.W. Koch, H. M Gibbs, G. Khitrova, and M. Oestreich, Phys. Rev. B **56**, 7076 (1997).
[9] E. Özbay, D.M. Bloom, D.H. Chow, and J.N. Schulman, IEEE Electron Device Lett. **14**, 400 (1993).
[10] J.T. Olesberg, W.H. Lau, M.E. Flatté, C. Yu, E. Altunkaya, E.M. Shaw, T.C. Hasenberg, and T.F. Boggess, Phys. Rev. B **64**, 201301 (2001).
[11] W.H. Lau and M.E. Flatté, Appl. Phys. Lett. **80**, 1683 (2002).
[12] L. Vervoort, R. Ferreira, and P. Voisin, Semicond. Sci. Technol. **14**, 227 (1999).
[13] O. Krebs and P. Voisin, Phys. Rev. Lett. **77**, 1829 (1996).
[14] W.H. Lau, J.T. Olesberg, and M.E. Flatté, Phys. Rev. B **64**, 161301 (2001).
[15] M.I. D'yakonov and V.Yu. Kachorovskii, Sov. Phys. Semicond. **20**, 110 (1986).
[16] Y. Ohno, R. Terauchi, T. Adachi, F. Matsukura, and H. Ohno, Phys. Rev. Lett. **83**, 4196 (1999).
[17] R. Kaspi, J. Cryst. Growth **201/202**, 864 (1999).
[18] R. Kaspi, J. Steinshnider, M. Weimer, C. Moeller, and A. Ongstad, J. Cryst. Growth **225**, 544 (2001).
[19] D.H. Chow, R.H. Miles, and A.T. Hunter, J. Vac. Sci. Technol. B **10**, 888 (1992).
[20] G. Tuttle, H. Kroemer, and J.H. English, J. Appl. Phys. **67**, 3032 (1990).
[21] J. Steinshnider, M. Weimer, R. Kaspi, and G.W. Turner, Phys. Rev. Lett. **85**, 2953 (2000).
[22] M. Ebrahimzadeh, P.J. Phillips, and S. Das, Appl. Phys. B: Lasers Opt. **72**, 793 (2001).
[23] T_1 depends strongly on excess energy (Ref. 10) in (001) InAs/GaSb superlattices due to the relaxation of electron spins prior to carrier thermalization with the lattice. Although the low band gap of the (110) InAs/GaSb superlattice studied here (240 meV at 77 K) together with the limited tuning range of our OPO prevented studies of the excess energy dependence of T_1 in the (110) superlattice, since the spin lifetime we have observed (18 ps) is considerably longer than the carrier-lattice thermalization time (1–2 ps), no dependence of T_1 on excess energy is expected.

[24] The energy of injected electrons is estimated using the calculated effective masses of electrons and holes, which are similar in these short period InAs/GaSb superlattices.
[25] *Optical Orientation*, edited by F. Meier and B. P. Zakharchenya (North-Holland, New York, 1984).
[26] J.M. Kikkawa and D.D. Awschalom, Phys. Rev. Lett. **80**, 4313 (1998).
[27] A. Tackeuchi, O. Wada, and Y. Nishikawa, Appl. Phys. Lett. **70**, 1131 (1997).
[28] R. Terauchi, Y. Ohno, T. Adachi, A. Sato, F. Matsukura, and A. Tackeuchi, H. Ohno, Jpn. J. Appl. Phys., Part 1 **38**, 2549 (1999).
[29] T.F. Boggess, J.T. Olesberg, C. Yu, M.E. Flatté, and W.H. Lau, Appl. Phys. Lett. **77**, 1333 (2000).
[30] K.C. Hall, S.W. Leonard, H.M. van Driel, A.R. Kost, E. Selvig, and D.H. Chow, Appl. Phys. Lett. **75**, 4156 (1999).
[31] C.A. Hoffman, J.R. Meyer, E.R. Youngdale, F.J. Bartoli, and R.H. Miles, Appl. Phys. Lett. **63**, 2210 (1993).
[32] G. Bir, A. Aronov, and G. Pikus, Zh. Éksp. Teor. Fiz. **69** 1382, (1975) [Zh. Eksp. Teor. Fiz. **42**, 705 (1976)].
[33] J. Wagner, H. Schneider, D. Richards, A. Fischer, and K. Ploog, Phys. Rev. B **47**, 4786 (1993).
[34] A. Vinattieri, J. Shah, T.C. Damen, K.W. Goossen, L.N. Pfeiffer, M.Z. Maialle, and L.J. Sham, Appl. Phys. Lett. **63**, 3164 (1993).
[35] R.J. Elliott, Phys. Rev. **96**, 266 (1954).
[36] Y. Yafet, Solid State Phys. **14**, 1 (1963).
[37] J.-N. Chazalviel, Phys. Rev. B **11**, 1555 (1975).
[38] J. Steinshnider, J. Harper, M. Weimer, C.-H. Lin, S.S. Pei, and D.H. Chow, Phys. Rev. Lett. **85**, 4562 (2000).
[39] R.M. Feenstra, D.A. Collins, D.Z.-Y. Ting, M.W. Wang, and T.C. McGill, Phys. Rev. Lett. **72**, 2749 (1994).
[40] A.Y. Lew, S.L. Zuo, E.T. Yu, and R.H. Miles, Appl. Phys. Lett. **70**, 75 (1997).
[41] M.W. Wang, D.A. Collins, T.C. McGill, R.W. Grant, and R.M. Feenstra, J. Vac. Sci. Technol. B **13**, 1689 (1995).